From Layered Double Hydroxide to Spinel Nanostructures: Facile Synthesis and Characterization of Nanoplatelets and Nanorods

Genban Sun,[†,‡] Lingna Sun,[†] He Wen,[†] Zhiqian Jia,[‡] Kunlin Huang,[‡] and Changwen Hu*[,†]

The Institute for Chemical Physics and Department of Chemistry, Beijing Institute of Technology, Beijing 100081, P.R. China, and College of Chemistry, Beijing Normal University, Beijing 100875, P.R. China

Received: February 13, 2006; In Final Form: May 13, 2006

Mg−Al spinel ($MgAl_2O_4$) nanorods and nanoplatelets transformed from Mg−Al layered double hydroxide (Mg−Al-LDHs) were synthesized via a combined hydrothermal method and calcination route using Al$(NO_3)\cdot 9H_2O$ and $Mg(NO_3)_2\cdot 6H_2O$ as raw materials. The nanorods and nanoplatelets were characterized by means of physical techniques, including powder X-ray diffraction (XRD), transmission electron microscopy (TEM), high-resolution transmission electron microcopy (HRTEM), selected-area electron diffraction (SAED), Fourier transform infrared spectra (FT-IR), thermogravimetric (TG), and nitrogen adsorption−desorption isotherms. XRD patterns reveal that the Mg−Al-LDHs nanostructures were obtained under a hydrothermal reaction temperature of 200 °C and Mg−Al spinel nanostructures were fabricated via calcination of the Mg−Al-LDHs nanostructures at 750 °C. It can be seen from TEM that the sizes of the Mg−Al-LDHs nanoplatelets were about 20−40 nm and the diameters of the $MgAl_2O_4$ nanorods were ca. 6 nm. The HRTEM images indicate that the crystal lattice spaces of the $MgAl_2O_4$ nanorods and nanoplatelets are 0.282 and 0.287 nm, respectively.

Introduction

Layered double hydroxides (LDHs), a family of ionic lamellar solids, can be incorporated with various metal cations, such as Mg^{2+}, Zn^{2+}, Ni^{2+}, Fe^{2+}, Al^{3+}, Fe^{3+}, and Gd^{3+}, into the hydroxide layers and intercalated with many inorganic anions, such as Cl^-, CO_3^{2-}, and NO_3^-, into the interlayer spacing, as well as DNA and drug molecules, so the synthesis of these LDHs nanomaterials is a systematic and challenging task, which can promote the progress of host−guest chemistry and physics.[1] Low-dimension nanostructured metal oxides, especially spinel-type oxides, AB_2O_4, are of great scientific interest due to their unique properties, such as mechanical strength, electronic properties, photonic efficiency, catalysis, and sensitivity. Therefore, these materials have important applications in various areas including fabricating nanodevices,[2] sensors,[3] photoelectronics,[4] and electronics,[5] catalysts for many reactions, including pollution control (NOx and SO_2 reduction), and oxidation of CO and hydrocarbons.[6a−e] Mg−Al spinel ($MgAl_2O_4$) possess two kinds of active centers, which are acidic and alkaline centers, as well as steady structure. Thus, the catalysis of nanostructured $MgAl_2O_4$ has initiated the current worldwide intense research on the field of catalytic synthesis of fined chemicals. Moreover, $MgAl_2O_4$ spinel is one of the most promising advanced ceramic materials which have high melting point, high resistance to chemical attack, high strength at elevated temperatures, and low electric loss. Therefore, it is also a good candidate material for microstructural design suitable for high-temperature applications.[7] Appropriate spinel composition may improve hot strength and slag resistance of an alumina−spinel composite ceramic.[8,9] The processing of spinel powders and its bulk materials have been extensively studied.[10−12] However, to the best of our knowledge, until now, there are few reports on low-dimension nanostructured Mg−Al-LDHs and complex oxides materials. For example, $MgAl_2O_4$ spinel nanowires have been obtained by a high-temperature route (≥1350 °C) reported by Wu et al.[13] Very recently, Valdes-Solis et al. invented a silica xerogel template route to prepare spinel nanoparticles.[14] Xu et al. reported preparation strategy of the LDHs nanoparticles in aqueous solution.[15] Here, we report the synthesis of Mg−Al-LDHs and Mg−Al spinel nanorods with diameters of 4−8 nm and nanoplatelets with a width of 30 nm via a simple hydrothermal method at the temperature as low as 200 °C and a simple calcination at 750 °C for 5 h in air. And the influence of the reaction time and temperature on the morphologies of the products was also explored. In addition, these spinel nanomaterials can exhibit relatively higher values of the BET surface area due to their nanostructures[6a,16] and we speculate that the spinel nanorods and nanoplatelets should exhibit outstanding catalysis properties, which may be applied as novel oxidic nanocatalysts.[6e,14]

Experimental Section

Synthesis. To synthesize a typical Mg−Al-LDHs nanostructure via a hydrothermal route, 0.02 mol of Al$(NO_3)\cdot 9H_2O$ and 0.01 mol of $Mg(NO_3)_2\cdot 6H_2O$ were dissolved in 50 mL of deionized water with magnetic stirring. A desired amount of aqueous ammonia (13.25%) was added to this mixed solution to control the pH value of about 11.3−12.8. The resulting lacteous mixture was stirred for at least 30 min to become homogeneous, and then it was transferred into an 80 mL Teflon-lined stainless steel autoclave. After the vessel was sealed, it was statically placed in an oven and heated at 200 °C (or 180 °C) for 20 h [or 5 days]. The suspension thus obtained was allowed to cool to room temperature naturally, and then a mass of the white precipitate was obtained after centrifugation and

* To whom correspondence should be addressed. E-mail: gbsun@bnu.edu.cn (G. Sun); cwhu@bit.edu.cn (C. Hu). Tel: +86-10-68912667. Fax: +86-10-62828869.

[†] Beijing Institute of Technology.

[‡] Beijing Normal University.

10.1021/jp060916d CCC: $33.50 © 2006 American Chemical Society
Published on Web 06/17/2006

TABLE 1: Summary of the Main Results on the Products Obtained under Different Preparation Conditions and Textural Characterization of the Products

as-prepared samples	formulation detected by XRD	preparation conditions	morphologies
sample 1	Mg−Al-LDHs[a] $Al(OH)_3$[b]	hydrothermal process at 180 °C for 20 h	rodlike
sample 1′	cubic $MgAl_2O_4$[a] Al_2O_3[b]	sample 1 was calcined at 750 °C for 5 h	rodlike
sample 2	Mg−Al-LDHs	hydrothermal process at 200 °C for 20 h	platelet-like
sample 2′	cubic $MgAl_2O_4$	sample 2 was calcined at 750 °C for 5 h	rodlike

washed several times with absolute ethanol and distilled water. Finally, the products were dried in a vacuum oven at 60 °C for 12 h.

To synthesize a typical rod- or platelet-like Mg−Al complex oxide ($MgAl_2O_4$), the Mg−Al-LDHs nanorod or nanoplatelet was calcined at 750 °C for 5 h in air with a heating rate of 5 °C·min^{-1}. The main results of the products obtained under different preparation conditions are shown in Table 1, and the superscripts "a" and "b" in Table 1 represent the predominant phase and minor phase in the final product.

Characterization. The composition and phase purity of the as-synthesized samples were analyzed by XRD with monochromatized Cu Kα incident radiation by a Shimadzu XRD-6000 operated at 40 kV voltage and 50 mA current. XRD patterns were recorded from 5° to 80° (2θ) with a scanning step of 0.02°. The size distribution, morphologies, and SAED patterns of the Mg−Al-LDHs and spinel format were characterized by transmission electron microscopy (TEM, Hitachi, Model H-800, 200 kV and HRTEM, JEOL, JEM-2010, 200 kV). FT-IR spectra were recorded on a Nicolet MAGNA-IR 560 spectrometer with a wide-band MCT liquid-nitrogen-cooled detector and a KBr beam splitter. TG curves were recorded on TA2000 with a calefactive speed of 10 °C/min in an Ar atmosphere. The nitrogen adsorption−desorption isotherm and Barrett−Joyner−Halenda (BJH) methods were analyzed on a Micromeritics ASAP 2010 system accelerated surface area and porosimetry system.

Results and Discussion

1. Powder X-ray Diffraction Patterns (XRD) of the Products. The XRD patterns of the as-obtained products are shown in Figure 1a. The patterns 1, 1′, 2, and 2′ were the XRD of samples 1, 1′, 2, and 2′ described in Table 1, respectively. From Figure 1a, as all the peaks of the patterns are well-indexed, it can be considered that the as-obtained samples demonstrate a good crystallinity and no other impurities were observed in the products. Patterns 1 and 2 in Figure 1a show that samples 1 and 2 are the typical XRD patterns of analogous Mg−Al-LDHs materials (International Center for Diffraction Data (ICDD), PDF files No. 43-0071). The schematic diagram for the structure of Mg−Al-LDHs viewed from the [111] direction is shown in Figure 1b, which also indicates the layered structure. From its standard XRD data, we can also conclude that the molar rate of Mg to Al is 2:1, and a small quantity of $Al(OH)_3$ (▼ in pattern 1 in Figure 1a) was also observed in sample 1. It indicates that hydrothermal process at 180 °C for 20 h cannot make all raw material transform into Mg−Al-LDHs and it also shows that a little of Al_2O_3 (∗ in XRD pattern 1′ in Figure 1a) exists in sample 1′ obtained by hydrothermal process at 180 °C for 20 h and calcination at 750 °C for 5 h. But when the hydrothermal temperature was increased to 200 °C, $Al(OH)_3$ and Al_2O_3 were almost not observed in coexistence with samples 2 and 2′ (see patterns 2 and 2′ in Figure 1a). In Figure 1a, pattern 2 shows the three strongest peaks are (003), (006), and (009), which further confirm the layer structure of the Mg−Al-LDHs materials shown in Figure 1b.[17,18] The samples 1′ and 2′ exhibit a spinel structure from XRD patterns (patterns 1′ and 2′ in Figure 1a). The diffraction peaks of (111), (220), (311), (400), (511), and (440) are clearly distinguishable, and all of them can be readily indexed to a pure face centered cubic (fcc) phase of $MgAl_2O_4$ [space group: $Fd3m$(227)] with lattice constant $a = 8.08$ Å.[17] The lattice constants of nanostructured Mg−Al complex oxide are consistent with those of bulk $MgAl_2O_4$ (ICDD, PDF files No. 82-2424). In addition, all peaks are obviously wider than those obtained by general methods. The average diameters of the nanoplatelets (sample 2) have been calculated to be 34 nm by employing the Scherrer equation: $D = 0.94\lambda/B\cos\theta$, where B is the full width at half-maximum of the XRD peaks, θ is the angle of diffraction, and λ is the wavelength of the X-rays, in well agreement with those observed by TEM.

2. Morphologies of the Typical Nanostructures. The typical low-magnification TEM images of the Mg−Al-LDHs and the $MgAl_2O_4$ spinel obtained by hydrothermal process at 200 °C for 20 h are shown in Figures 2a and 2b. Figure 2a indicates that the morphologies of Mg−Al-LDHs are the hexagonal nanoplatelets with widths of 30−60 nm and the size distribution is fairly narrow. However, the morphologies of Mg−Al complex oxides are nanorods with diameters of 4−8 nm and lengths of 100−400 nm (see Figure 2b). Since the size and shape of the crystal are the function of hydrothermal time and temperature,[19] different morphologies and sizes of this complex should be obtained by adjusting the hydrothermal reaction time. When the hydrothermal reaction time was prolonged to 5 days, the products consisted mainly of the well-crystallized hexagonal nanoplatelets as shown in Figures 2c and 2d. From these two figures, we observe that the particle sizes of the Mg−Al-LDHs nanoplatelets (Figure 2c) are about 40 nm, but the particle sizes in width of the Mg−Al spinel nanoplatelets (Figure 2d) obtained after calcination at 750 °C for 5 h are 20−110 nm. In addition, SAED patterns inserted in Figures 2b and 2d show clear diffuse rings, which reveal that both the nanoplatelets and the nanorods can be indexed to cubic $MgAl_2O_4$ polycrystals. Then the Mg−Al-LDHs are also polycrystals, analogically (see the SAED patterns inserted in Figures 2a and 2c).

To further study the fine spinel structure of the nanorods and the nanoplatelets, HRTEM combined with a fast Fourier transform (FFT) analysis technique was employed. The clear lattice fringes in the HRTEM images confirm the high crystallization of the nanorods and the nanoplatelets (Figure 3). Different from previous reports,[13] in which the spinel nanowire grows along the [111] direction, in our case the as-prepared nanorods were found growing along the direction of [100] but the growth of $MgAl_2O_4$ nanoplatelets was terminated at the {110} planes, which were predicted to have the lowest surface energy.[20] In Figure 3a, all the spacing, either two adjacent horizontal or vertical lattice planes, is 0.282 nm. Combined with the results of FFT (the inset of Figure 4a, the electron bundles incidence direction defined B is [001]), the crystal structure of $MgAl_2O_4$ (shown in Figure 3c), and XRD analysis, they are found to correspond to the {220} and {$2\bar{2}0$} atomic lattice planes of the nanorods. As shown in Figures 3b and 3d (B is [111] direction), the nanoplatelet with growth direction along [110] exists with d_{220} of 0.287 nm. The lattice parameters of these

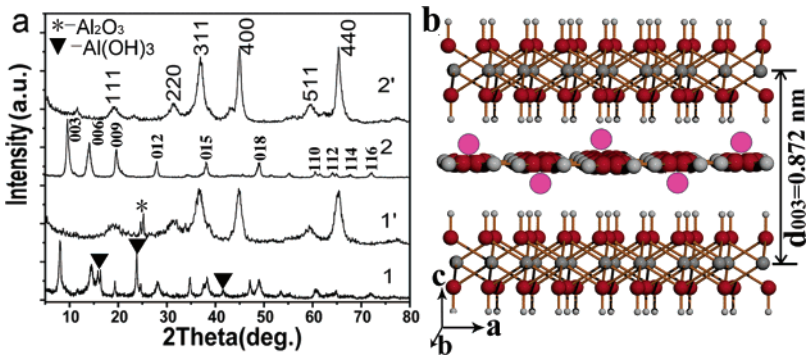

Figure 1. (a) XRD patterns of the products; (b) schematic diagram for the structure of Mg−Al−NO_3-LDHs viewed from the [111] direction: the large gray, medium gray, small gray, red, and pink spheres are H, Mg, Al, O, and $-NO_3$, respectively.

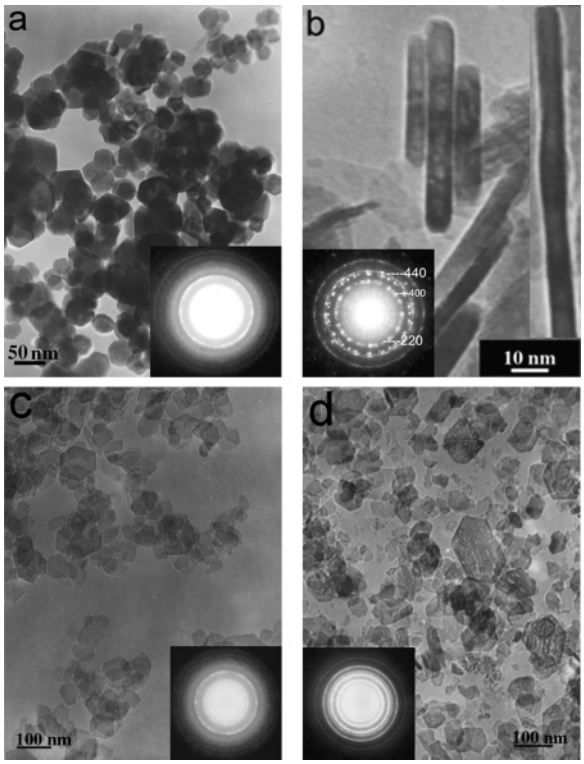

Figure 2. TEM images of the as-prepared products: (a) sample 2 obtained by only hydrothermal process at 200 °C for 20 h; (b) sample 2′ obtained by hydrothermal process at 200 °C for 20 h and then calcination at 750 °C for 5 h; (c) sample obtained by only hydrothermal process at 200 °C for 5 days; and (d) sample obtained by hydrothermal process at 200 °C for 5 days and then calcination at 750 °C for 5 h. The inserted TEM image of part (b) is typical $MgAl_2O_4$ nanorods; the other insets are SAED patterns of the nanoplatelets and the nanorods.

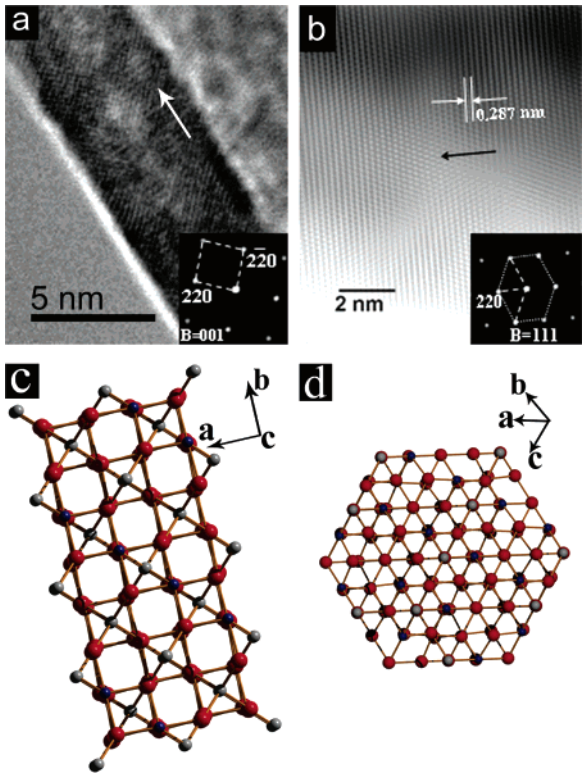

Figure 3. HRTEM images of a typical spinel (a) nanorod of sample 2 ($d_{220} = d_{2\bar{2}}20 = 0.282$ nm) and (b) nanoplatelet of sample 2′ ($d_{220} = 0.287$ nm); the insets of (a) and (b) are two-dimensional FFT analysis of the nanorod and nanoplatelet, respectively. (c) and (d) schematic diagram for a partially filled unit cell of spinel AB_2O_4 viewed from the direction of [001] and [111]: gray, blue, and red cells are Mg, Al, and O, respectively.

two kinds of products with different growth directions verify that the as-prepared nanomaterials possess the same crystal structure.

3. Effect of the Hydrothermal Reaction Temperature (*T*) and Reaction Time (*t*). Since the hydrothermal reaction temperature (*T*) and reaction time (*t*) can significantly influence the size and shape of the crystal,[19] we consider them the key factors in this reaction system. For comparison, we performed the experiment under hydrothermal conditions at 180 °C but kept other conditions the same as the experiment under hydrothermal process at 200 °C. Figures 4a−4d show the TEM images of Mg−Al-LDHs and Mg−Al complex oxides nanostructures obtained under these conditions. As shown in Figure 4a, when *T* is 180 °C and *t* is 20 h, the resulting Mg−Al-LDHs sample mainly consists of nanorods with diameters of about 14 nm and lengths of 60−200 nm. However, after calcination at 750 °C for 5 h, the TEM images become a little illegible but the rodlike morphologies remain (see Figure 4b). When $t = 5$ days, large-scale cubic and hexagonal nanoplatelets of Mg−Al-LDHs including several rodlike ones were obtained (Figure 4c). As shown in Figure 4c, the diameters of the nanoplatelets are ca. 30 nm. However, the TEM image in Figure 4d shows the resulting samples obtained by calcination of the Mg−Al-LDHs (shown in Figure 4c) at 750 °C for 5 h. It can be seen from Figure 4d that the amounts of the $MgAl_2O_4$ nanorods are increased and their dimensions are 100−150 nm long and 5−10 nm wide. The observed SAED rings (see the inset of Figure 4d) are converted to the lattice spacings of 0.288, 0.246, and 0.204 nm, which are nicely indexed to the {220}, {311}, and {400} planes of the fcc, respectively. This is in complete agreement with the above conclusion from the XRD results. When *T* is 140 °C and *t* is 20 h, the morphologies of Mg−Al-

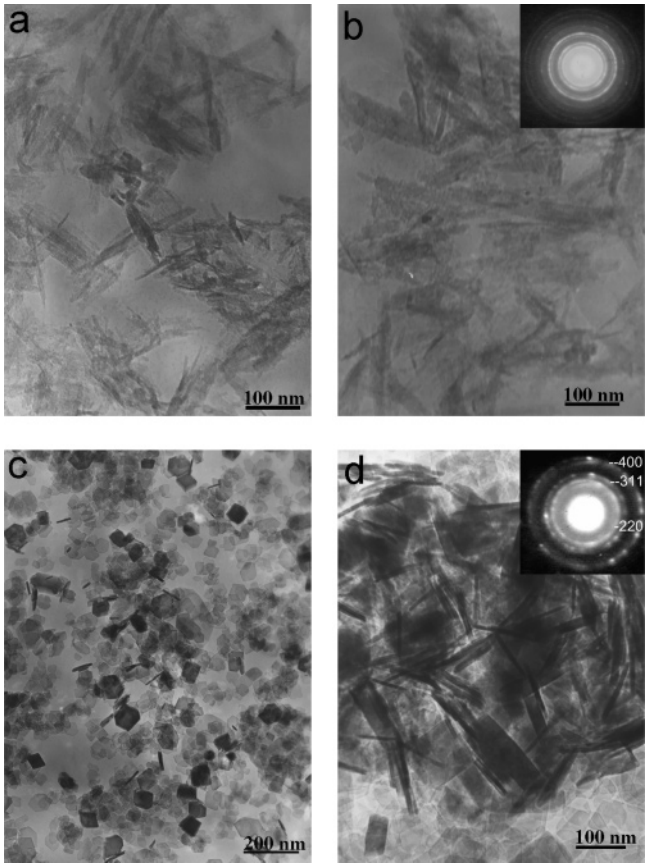

Figure 4. Morphologies of the products: (a) sample 1 obtained by only hydrothermal process at 180 °C for 20 h, (b) sample 1′ obtained by hydrothermal process at 180 °C for 20 h and then calcination at 750 °C for 5 h, (c) sample obtained by only hydrothermal process at 180 °C for 5 days, and (d) sample obtained by hydrothermal process at 180 °C for 5 days and then calcination at 750 °C for 5 h. The insets of (b) and (d) are SAED patterns of the nanorods and the nanoplatelets.

LDHs with compositions of NO_3^- are sheetlike with the lateral dimensions in the range of 20−70 nm (see Figure S1a in Supporting Information), and when Mg−Al-LDHs nanoplatelets obtained under this condition were calcined at 750 °C, the spinel nanorods with a diameter of 10 nm were obtained (see Figure S1b and Figure S1c in Supporting Information). Furthermore, based on the effects of the hydrothermal reaction temperature and reaction time, we can speculate the formation mechanism for the nanostructures is similar to that recently reported by Xu et al.[15] First, before the hydrothermal process in the suspension, there are many aggregates with the sizes of 1−10 μm that contain many sheetlike LDHs nanocrystallites in each aggregate. Then, the LDHs nanoplatelets were obtained under hydrothermal conditions. Finally, the spinel nanostructures formed after calcination. But the morphology of $MgAl_2O_4$ spinel changed with the different hydrothermal time of the Mg−Al-LDH nanoplatelets. If the Mg−Al-LDH nanoplatelets were obtained with the hydrothermal temperature of 200 °C and the time of 20 h, the resultant products of the spinel mainly consist of rodlike nanostructures because of the shrinking of the nanoplatelets during calcination; if the hydrothermal time is 5 days, the spinel will keep the sheetlike structures of the Mg−Al-LDHs due to the LDHs being completely crystallized.

4. Fourier Transform Infrared (FT-IR) Spectra and Thermal Stability of the Nanostructures. FT-IR spectra of the samples 1, 1′, 2, and 2′ are shown in Figure 5. The spectral peaks provide vibrational information for the functional groups in the samples, which is very important for characterizing the

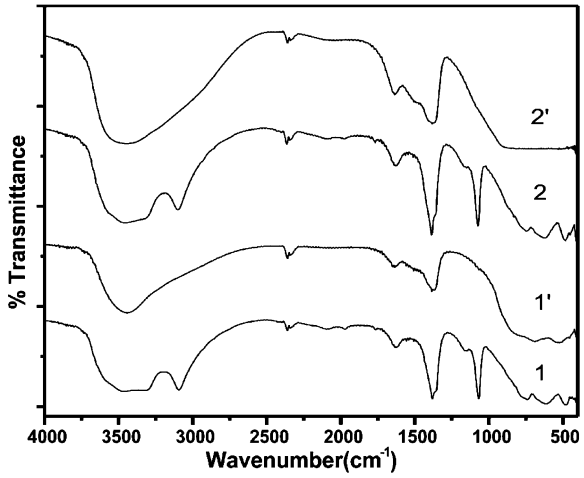

Figure 5. FT-IR of samples 1, 1′, 2, and 2′.

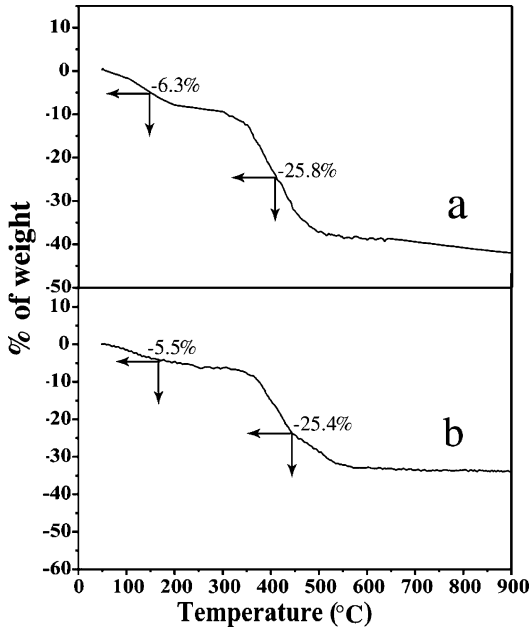

Figure 6. TG curves of (a) sample 1 and (b) sample 2.

structure and composition of the materials. From Figure 5, it can be clearly seen that there is nearly a one-to-one correspondence of the major peaks among the spectra of samples 1 and 2, as well as samples 1′ and 2′. In addition, the peak positions are close despite very small shifts. This indicates that the functional groups and structures are similar in the materials. The small spectral shifts may be caused by the change from a fcc structure to a nanostructure. We conclude that Mg−Al-LDHs have six characteristic peaks: the stretching vibration of O−H in the crystallization water (generally appearing at 3300−3540 cm^{-1}), the symmetric stretching vibration of the interbedded −OH (narrow peak at 3084 cm^{-1}), the bending vibration of O−H in the crystallization water (1623 cm^{-1}), the bending vibration of N−O (1375 cm^{-1}), the symmetric stretching vibration of the interbedded N−O (1045 cm^{-1}), and the finger peaks of the lattice vibration modes of Mg−O and Mg−OH (400−900 cm^{-1}).[21] As shown in Figure 6, when samples 1 and 2 were calcined at 750 °C for 5 h in air, two narrow peaks at 3084 and 1045 cm^{-1} (the interbedded $-NO_3$ and −OH) disappeared, which indicated that the Mg−Al complex oxides (sample 1′ and 2′) came into being. Moreover, in spinel formation, two small and broad peaks at 631−511 cm^{-1}

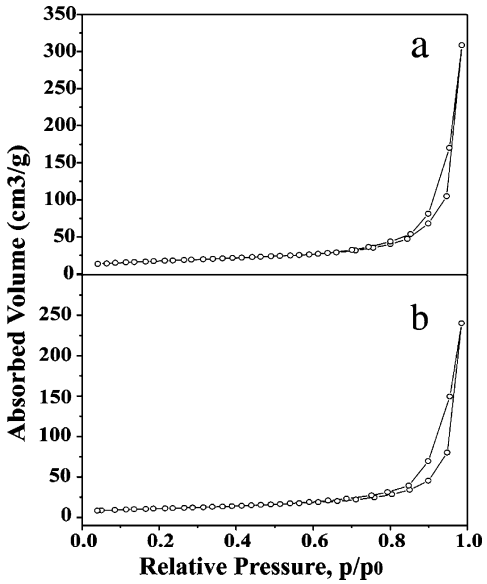

Figure 7. Nitrogen isotherms of the nanostructures: (a) sample 2; (b) sample 2′.

appeared due to AlO_6 group building up of spinel formation, and their intensity increased with the higher temperature.[22]

Thermal analysis experiments were employed to further characterize the thermal stability of the as-prepared nanomaterials in combination with XRD studies, and the TG data for the samples 1 and 2 protected by an Ar atmosphere are presented by curves a and b in Figure 6. For samples 1 and 2, the process for weight loss consists of two remarkable steps in the TG curve from room temperature up to ca. 900 °C, including desorption of water physisorbed on the external surface of the crystallites and removal of water intercalated in the interlayer galleries and dehydroxylation of the lattice, respectively. From curve a, it can be clearly seen that the crystallization water and physisorbed water in sample 1 stripped down at 147.3 °C and the weight loss was 6.3 wt %. In the process from 363.2 to 441.2 °C, sample 1 decomposed into $MgAl_2O_4$ and a little Al_2O_3. This weight loss was about 25.8 wt % and the temperature was 376.7 °C, which is when the water intercalated in the interlayer galleries was stripped down and the dehydroxylation of the lattice took place. From curve b, the first weight loss for sample 2 was 5.5 wt % and the temperature was 155.3 °C, and the second weight loss was 25.4 wt % and the temperature was 429 °C, the sample then decomposing into $MgAl_2O_4$; these values are in good agreement with the theoretical values. The weight loss values of sample 1 are higher than those for sample 2, which is ascribed to the degree of crystallization and a few aluminum hydroxides in sample 1. This result is consistent with the XRD and FT-IR data discussed above. When the temperature is increased to greater than 900 °C, there is no weight loss in either sample; it confirms that the spinel nanostructures are very stable under high temperature.

5. Nitrogen Isotherms of the Nanostructures. The isotherms of nitrogen adsorption and desorption at 77 K for the nanostructures prepared by only the hydrothermal process at 200 °C for 20 h (sample 2) and by the hydrothermal process at 200 °C for 20 h and then calcination at 750 °C for 5 h (sample 2′) are plotted in Figure 7. The isotherms can be categorized as type IV, with distinct hysteresis loops observed in the range of 0.70−0.90 p/p_0 (Figure 7a) and 0.61−0.96 p/p_0 (Figure 7b), respectively. Using these isotherms, it is possible to calculate the values of the BET surface area (S_{BET}); S_{BET} values of sample 2 and sample 2′ are 42.62 and 80.40 m^2/g, respectively. From Figure 7a, it can be observed that the materials of a diminutive particle size exhibit a capillary condensation step, which is especially marked in the case of Mg−Al-LDHs and $MgAl_2O_4$ at relative pressure, $p/p_0 = 0.70-0.90$ and $p/p_0 = 0.61-0.96$, respectively. The pore size distribution analysis of the sample shows pore diameters are around 30 nm, which are attributed to the interparticle spaces.[23] TEM inspection (Figure 2) also indicates that the case of Mg−Al-LDHs should be attributed to the existence of a layered structure and the case of $MgAl_2O_4$ should be ascribed to the aggregation of small nanoparticles, which favors the capillary condensation, but not to the existence of structural porosity. Because the particle sizes of sample 2′ are much smaller than those of sample 2, the S_{BET} of sample 2′ is larger than that of sample 2.

Conclusions

In summary, different Mg−Al-LDHs nanostructures had been synthesized via a simple hydrothermal route and $MgAl_2O_4$ spinel nanostructures had been prepared by simple calcination of Mg−Al-LDHs at low temperature in air. With careful control of the fundamental experimental parameters including the reaction time and the hydrothermal reaction temperature, the morphologies of rods and hexagonal platelets with different sizes were efficiently obtained, respectively. We speculate that it will be a general, innovative, and low-cost method for preparing series of spinel nanosized mixed oxide catalysts. The thermal stability and the values of the BET surface area of the nanostructures were explored, and the specific surface areas obtained by the hydrothermal method are considerably larger than those attained by other conventional methods.

Acknowledgment. This work was supported by the Natural Science Foundation of China (NSFC, No. 20331010, 90406002) and Specialized Research Fund for the Doctoral Program of Higher Education (SRFDP, No. 20030007014).

Supporting Information Available: TEM images of Mg−Al-LDHs nanoplatelets and $MgAl_2O_4$ nanorods obtained under hydrothermal conditions of 140 °C for 20 h and in succession calcination at 750 °C for 5 h, respectively. This material is available free of charge via the Internet at http://pubs.acs.org.

References and Notes

(1) (a) Desigaux, L.; Belkacem, M. B.; Richard, P.; Cellier, J.; Léone, P.; Cario, L.; Leroux, F.; Taviot-Guého, C.; Pitard, B. *Nano Lett.* **2006**, *6*, 199. (b) Carriazo, D.; Domingo, C.; Martín C.; Rives, V. *Inorg. Chem.* **2006**, *45*, 1243.

(2) Ajayan, P. M.; Redlich, P.; Rühle, M. *J. Microsc.* **1997**, *185*, 275.

(3) Pena, M. A.; Fierro, J. L. G. *Chem. Rev.* **2001**, *101*, 1981.

(4) Hu, J.; Li, L.; Wang, W.; Manna, L.; Wang, L.; Alivisatos, A. P. *Science* **2001**, *292*, 2060.

(5) Hu, J.; Odom, T. W.; Lieber, C. M. *Acc. Chem. Res.* **1999**, *32*, 435.

(6) (a) Zarur, A. J.; Ying, J. Y. *Nature* **2000**, *403*, 65. (b) Jansson, J.; Palmqvist, A.; Fridell, E.; Skoglundh, M.; Österlund, L.; Thormählen, P.; Langer, V. *J. Catal.* **2002**, *211*, 387. (c) Sloczynski, J.; Janas, J.; Machej, T.; Rynkowski, J.; Stoch, J. *Appl. Catal., B* **2000**, *24*, 45. (d) Chen, L. Y.; Horiuchi, T.; Mori, T. *React. Kinet. Catal. Lett.* **2000**, *69*, 265. (e) Shen, S. C.; Hidajat, K.; Yu, L. E.; Kawi, S. *Adv. Mater.* **2004**, *16*, 541.

(7) White, K. W.; Kelker, G. P. *J. Am. Ceram. Soc.* **1991**, *74*, 1732.

(8) Ko, Y. C.; Chan, C. F. *J. Eur. Ceram. Soc.* **1999**, *19*, 2633.

(9) Ko, Y. C. *Ceram. Int.* **2002**, *28*, 805.

(10) Bratton, R. *J. Am. Ceram. Soc. Bull.* **1969**, *48*, 759.

(11) Wang, C. T.; Lin, L. S.; Yang, S. J. *J. Am. Ceram. Soc.* **1992**, *75*, 2240.

(12) Singh, V. K.; Sinha, R. K. *Mater. Lett.* **1997**, *31*, 281.
(13) Wu X. C.; Tao, Y. R.; Han, Z. J.; Zhang, B. D. *J. Mater. Chem.* **2003**, *13*, 2649.
(14) Valdes-Solis, T.; Marban, G.; Fuertes, A. B. *Chem. Mater.* **2005**, *17*, 1919.
(15) Xu, Z.; Stevenson, G.; Lu, C.; Lu, G.; Bartlett, P.; Gray, P. *J. Am. Chem. Soc.* **2006**, *128*, 36−37.
(16) Praserthdam, P.; Silveston, P. L.; Mekasuwandumrong, O.; Pavarajarn, V.; Phungphadung, J.; Somrang, P. *Cryst. Growth Des.* **2004**, *4*, 39.
(17) Li, F.; Liu, J. J.; Evans, D. G.; Duan, X. *Chem. Mater.* **2004**, *16*, 1597.
(18) Schutz, A.; Biloen, P. *J. Solid State Chem.* **1987**, *68*, 360.
(19) Kruissink, E. C.; Reijen, L. L. V.; Ross, J. R. H. *J. Chem. Soc., Faraday Trans.* **1981**, *77*, 649.
(20) (a) Davies, M. J.; Parker, S. C.; Watson, G. W. *J. Mater. Chem.* **1994**, *4*, 813. (b) Song, Q.; Zhang, Z. J. *J. Am. Chem. Soc.* **2004**, *126*, 6164.
(21) Titulaer, M. K.; Jansen, J. B. H.; Geus, J. W. *Clays Clay Miner.* **1994**, *42*, 249.
(22) Zawrah, M. F. *Mater. Sci. Eng. A* **2004**, *382*, 362−370.
(23) Hu, J. S.; Ren, L. L.; Guo, Y. G.; Liang, H. P.; Cao, A. M.; Wan, L. J.; Bai, C. L. *Angew. Chem., Int. Ed.* **2005**, *44*, 1269.